



Thermohydraulics of TiO₂/Water Nanofluid in a Round Tube with Twisted Tape Inserts

Smith Eiamsa-ard¹ · Kunlanan Kiatkittipong²

Received: 16 April 2014 / Accepted: 19 January 2019 / Published online: 6 February 2019
© Springer Science+Business Media, LLC, part of Springer Nature 2019

Abstract

The influence of TiO₂ nanoparticles with different volume concentrations in water on heat transfer, friction and thermal performance is explored, and finite volume method is used to clarify the heat transfer in a tube inserted with twisted tape (TT). In the experiment, swirling tubes are generated by TT insert with the twisted ratio (y/w) of 3.0 in the range of Reynolds number between 5400 and 15,200. The mathematical modeling which involves the prediction of flow behaviors in a tube is also conducted. The concentration of nanofluid (ϕ) was varied from 0.07 % to 0.21 % by volume. The results revealed that TiO₂ nanoparticles suspended in water enhanced thermal conductivity, and movement of TiO₂ nanoparticles delivered energy exchange. Although an increase of TiO₂ concentration led to an increase in friction due to small particles suspending in fluid, the heat transfer and thermal performance could enhance significantly. As compared to pure water, the presence of TT with TiO₂ nanoparticles at $\phi = 0.07\%$, $\phi = 0.14\%$ and $\phi = 0.21\%$ indicated a 0.7 %, 1.7 % and 3.1 % higher thermal performance, respectively. With a higher Reynolds number, the thermal performance would be less pronounced due to high flow friction. From the experimental results, the understanding in relation to the effects of TiO₂ concentration and Reynolds number on Nusselt number (Nu), friction factor (f) and thermal performance factor (η) is presented for a wide range of thermophysics and heat transfer application.

Keywords Heat exchanger · Heat transfer enhancement · Nanofluid · Titania · Twisted tape

✉ Kunlanan Kiatkittipong
kunlanan.kia@kmitl.ac.th
Smith Eiamsa-ard
smith@mut.ac.th

¹ Department of Mechanical Engineering, Faculty of Engineering, Mahanakorn University of Technology, Bangkok 10530, Thailand

² Department of Chemical Engineering, Faculty of Engineering, King Mongkut's Institute of Technology Ladkrabang, Bangkok 10520, Thailand

1 Introduction

An efficiency of refrigeration, automotive and chemical process industries mainly depends on heat transfer enhancement of compact heat exchangers [1–4]. Swirl flow devices have been applied in order to promote turbulence which can improve heat transfer and reduce a heat exchanger size [5–9]. One of the widely used swirl flow devices is twisted tapes due to low cost and simple installation in the existing heat exchanger. The fluids containing innovative particles in nanometer, called nanofluid, are interesting approach to enhance heat transfer. The dispersed nanoparticles such as TiO_2 , Al_2O_3 and CuO were found to change the thermal properties of fluid such as thermal conductivity, heat transfer, friction factor, viscosity, specific heat and density of the base fluid [10–12]. Sharma et al. [13] found that the heat transfer coefficient in tube fitted with twisted tape inserts using 0.1 % v/v Al_2O_3 nanofluid was 23.7 % higher than those with pure water, and the maximum friction factor was 1.21 times over a plain tube. Sundar and Sharma [14] determined the convective heat transfer coefficient, thermal conductivity, viscosity and friction factor for twisted tape inserts with Al_2O_3 nanofluid at different volume concentrations and temperatures. 0.5 % v/v Al_2O_3 nanofluid with twist ratio of five provided the heat transfer coefficient of 33.5 % and friction factor of 1.096 times compared to those of the plain tube with pure water. Naik et al. [15] investigated the convective heat transfer and friction factor behaviors for a mixture between 70 % of water and 30 % of propylene glycol. The tube was equipped with twisted tapes, and CuO concentrations of 0.25 %, 0.1 % and 0.5 % by volume in fluid were studied. It was found that the convective heat transfer coefficient for 0.5 % CuO was around 76 % higher than for the base fluid at a particular Reynolds number, while the friction factor enhancement increased to up to 26.6 %. Suresh et al. [16, 17] studied a tube fitted with helical screw tape at different twist ratios ($y/w = 1.78, 2.44$ and 3) together with Al_2O_3 and CuO in laminar and transition flow regimes. The Nusselt number increased with a decrease in twist ratios. With a helical screw tape at twist ratio of 1.78, 2.44 and 3, the Nusselt number for Al_2O_3 /water nanofluid was 166.8 %, 128.7 % and 89.2 %, while the Nusselt number for CuO /water was 179.8 %, 144.3 % and 105.6 %, respectively. This indicated that CuO obviously outperformed Al_2O_3 in nanofluid. Wongcharee and Eiamsa-ard [18] found that the twisted tape with alternate axis insert exhibited 12.8 times more the heat transfer than the plain tube. When 0.7 % v/v CuO was added in water together with the twisted tape having alternate axis insert, the heat transfer increased up to 13.8 times over the plain tube. That is, the maximum thermal performance factor was 5.53. Later, Eiamsa-ard and Wongcharee [19] developed the device to enhance thermal performance factor by using dual twisted tapes and microfin tube together with CuO /water nanofluid. They observed that the combination of microfin tube and dual twisted tapes consistently showed superior thermal performance factor when compared with the tube with a single twisted tape as well as the microfin tube alone. Wongcharee and Eiamsa-ard [20] also examined the difference in rearrangement of the twisted tape coupled with corrugated tube between counter pattern and parallel pattern. 0.7 % CuO in water in corrugated tube with twisted tape in counter arrangement showed the best thermal performance factor of 1.57. As compared to the corrugated tube alone, corrugated tube together with twisted tape in counter arrangement provides over 2.67 times and 5.76 times more transfer rate

and friction factor, respectively. He et al. [21] examined the heat transfer of TiO₂ nanofluid in flowing through vertical tube. They found that the TiO₂ nanoparticles affected to an improvement of heat transfer coefficient, while pressure drop was still similar to that of base fluid. Regarding to the above studies, the role of twisted tape and nanofluid is still less clear. This work focuses on the characteristics of both TiO₂/water nanofluid and a twisted tape for greater understanding in heat transfer enhancement. The SST $k-\omega$ model (the QUICK scheme) was used to clarify streamline around the tube with twisted tape insert and temperature field. Additionally, the impact of TiO₂ concentration on Nu distribution, heat transfer, friction factor and thermal performance has been considered, and the empirical correlations are developed.

2 Theoretical Analysis

This work focuses on using TiO₂ as a working fluid together with a twisted tape in tube under the fully developed turbulent flow condition. The characteristics of heat transfer and pressure drop were studied, and Reynolds number and volume concentrations (ϕ) were considered. Moreover, the thermophysical properties of the nanofluid were as follows:

The density of nanofluid was evaluated from the following equation:

$$\rho_{nf} = (1 - \phi)\rho_{water} + \phi\rho_{np} \quad (1)$$

The specific heat of the nanofluid is calculated from:

$$c_{p,nf} = \frac{\phi\rho_{np}c_{p,np} + (1 + \phi)\rho_{water}c_{p,water}}{\rho_{nf}} \quad (2)$$

The thermal conductivity is determined by Maxwell model. Note that small amount of nanoparticles are non-interacting and properly disperse in liquid as shown in Eq. 3

$$\frac{k_{nf}}{k_{water}} = \frac{k_{np} + 2k_{water} + 2\phi(k_{np} - k_{water})}{k_{np} + 2k_{water} - \phi(k_{np} - k_{water})} \quad (3)$$

Viscosity of nanofluids is evaluated by the Einstein's formula.

$$\mu_{nf} = \mu_{water}(1 + \eta\phi) \quad (4)$$

where $\eta = 2.5$, as recommended for hard spheres.

The Reynolds number in a tube is given by

$$Re = \rho UD/\mu \quad (5)$$

where the mean velocity (U) of fluid was evaluated by using the existed rotameter.

The principal wall of the tube was heated by electrical heater served to be constant wall heat flux. The average wall temperature was evaluated by the measured temperatures of the sidewall. The rate of heat input, Q_{in} , to the tube wall is supposed to be

totally dissipated to the fluid flowing through the tube passage and raises its temperature from inlet bulk temperature (T_i) to exit bulk fluid temperature, (T_o). The rate of heat dissipated to the bulk fluid is shown below

$$Q_{in} = V \times I \quad (6)$$

Due to the radiation and convection heat losses, the heat supplied is set 5 to 8% higher than the heat absorbed by the fluid for thermal equilibrium test.

$$Q_{in} > Q_f \approx 5 \text{ to } 8\% \quad (7)$$

At the steady state, the rate of convective heat transfer is defined by where the rate of heat transfer absorbed by the fluid as shown below:

$$Q_f = Q_{conv} \quad (8)$$

where

$$Q_f = \dot{m}c_{p,f}(T_o - T_i) \quad (9)$$

The convection heat transfer can be expressed as:

$$Q_{conv} = hA(\tilde{T}_w - T_b) \quad (10)$$

whereas

$$T_b = (T_o + T_i)/2 \quad (11)$$

and

$$h = \dot{m}c_{p,f}(T_o - T_i)/A(\tilde{T}_w - T_b) \quad (12)$$

$$h_m = \Sigma h/15 \quad (13)$$

where h is the local heat transfer coefficient and is examined at the outer wall surface of the inner tube. The average local heat transfer coefficients were evaluated from 15 points where the positions of the thermocouples were 15 mm, 85 mm, 155 mm, 225 mm, 295 mm, 365 mm, 435 mm, 505 mm, 575 mm, 645 mm, 715 mm, 785 mm, 855 mm, 925 mm and 975 mm from the entrance of the test tube with 1000 mm in length. All the fluid thermophysical properties were calculated at the bulk mean temperature, T_b .

The average Nusselt number, Nu , is estimated as follows:

$$Nu = h_m D/k \quad (14)$$

The friction factors are evaluated from the pressure drop across the test tubes as follows:

$$f = 2\Delta P(D/L)/\rho U^2 \quad (15)$$

A difference of heat transfer coefficients between enhancement devices (twisted tape and TiO₂/water nanofluid) and plain tube with pure water can be made at equal pumping power. The thermal performance factor of the tube with enhancement devices was calculated as follows:

$$\eta = (Nu_t/Nu_p)/(f_t/f_p)^{1/3} \quad (16)$$

where thermal performance criteria, η , is defined as the ratio between the Nusselt number ratio (enhancement devices/plain tube) and the friction factor ratio (enhancement devices/plain tube).

3 Experimental Test Rig

A calm section was prepared at the length of 1200 mm. The tube with a diameter (D) of 19 mm and length (L) of 1000 mm was made from copper with a thickness (t) of 1.5 mm, and insulated to protect heat loss. The electrical heater wire was attached around the tube, and the electrical output power was controlled by a Variac transformer. Twisted tapes were made from aluminum strips with thickness of 0.8 mm, width of 18 mm (w) and pitch length (y) at twist ratios of $y/w = 3$. RTD Temperature data loggers with highly accurate calibrations are used to measure the inlet and outlet temperatures of the fluid. The fifteen type T thermocouples were attached on the sidewall of the tubes to measure the temperature variations around each tube cross section. 100% anatase TiO₂ was dispersed in water using ultrasonic vibrator for 5 h. 0.07%, 0.14% and 0.21% TiO₂ by volume were studied in the present work. The inlet fluid is set at the Reynolds number from 5400 to 15,200. The inlet bulk fluid at 26 °C from setting tank was transferred to the heat transfer test tube. During the heat transfer experiments, an electrical heater was applied to the bulk fluid along the test tube. For each experiment, at steady-state condition, the volumetric flow rate, temperature and pressure drop of the bulk fluid were collected. The average of inlet–outlet fluid and tube wall temperatures was considered for the characteristics of the flow and the Nusselt number. Manometers are used to measure pressure drop of the heat transfer test tube under an isothermal condition. The experiment was repeated three times to ensure the reproducibility of the results.

4 Mathematical and Numerical Method

The finite difference mathematical modeling was applied to solve the governing partial differential equations for swirling flows and boundary layer to predict the flow behavior in a tube. The major assumptions for conventional momentum and energy equations to model the heat transfer behavior in tube included twisted tape are: (1) the turbulent flow through the twisted tape, (2) the steady state and incompressible flow, (3) natural heat convection and heat radiation are neglected and (4) the ther-

mophysical properties of the fluid are temperature independence. According to above assumptions, the mathematical modeling with the governing differential equations is modeled to describe the fluid flow and heat transfer in round tubes with twisted tape inserts. The three-dimensional models of continuity, momentum and energy equations are employed. The time-averaging of Navier–Stokes equations for incompressible fluid in the Cartesian tensor notation with steady flow can be shown as following form:

Continuity equation:

$$\frac{\partial}{\partial x_i}(\rho u_i) = 0 \quad (17)$$

Momentum equation:

$$\frac{\partial(\rho u_i u_j)}{\partial x_j} = \frac{\partial p}{\partial x_i} + \frac{\partial}{\partial x_j} \left[\mu \left(\frac{\partial u_i}{\partial x_j} + \frac{\partial u_j}{\partial x_i} - \frac{2}{3} \delta_{ij} \frac{\partial u_k}{\partial x_k} \right) \right] + \frac{\partial}{\partial x_j} (-\rho \overline{u'_i u'_j}) \quad (18)$$

Energy equation:

$$\frac{\partial}{\partial x_i} [u_i(\rho E + p)] = \frac{\partial}{\partial x_j} \left(k_{eff} \frac{\partial T}{\partial x_j} \right), \quad E = h - \frac{p}{\rho} + \frac{u^2}{2} \quad (19)$$

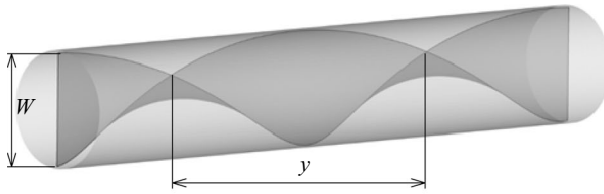
In the present numerical method solution, the finite volume technique was used to discrete incompressible Navier–Stokes equations with the time-independent and the turbulence model. QUICK for convective and central differencing numerical schemes for diffusive terms was applied.

SIMPLE algorithms for pressure–velocity coupling were used to determine the pressure field. Impermeable boundary condition has been applied over the tube wall. The turbulence intensity was kept constant at 10 % at the inlet. The computation had been finished based on a convergence criterion, where the normalized residual of the algebraic equation is less than the prescribed value of 10^{-6} . According to regular Cartesian elements, the flow in tube fitted with twisted tape at twist ratio, $y/w = 3.0$ for only 180° twist length, was presented in the form of the computational domain as shown in Fig. 1a, b. Grid-independent solution was reached for solutions on different grid levels, consisting of 5472 elements. The Reynolds numbers used for the computation were referred to the inlet values and set at 5000. The inlet temperatures were kept constant at 300 K, while the outer tube wall was maintained under a constant heat flux condition.

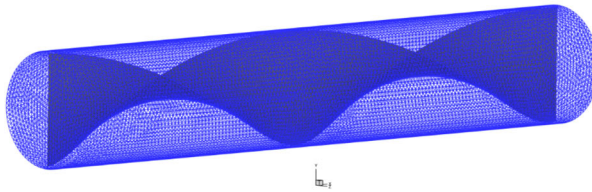
5 Experimental Results

5.1 Flow Structure

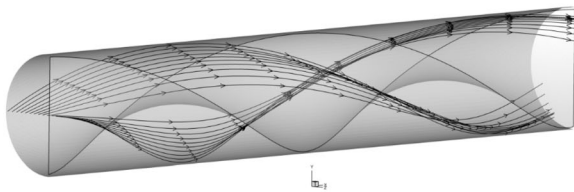
Streamline around the tube with twisted tape insert was predicted by SST $k-\omega$ model using the QUICK scheme as depicted in Fig. 1c. The swirl flow in mainly forward direction is generated around the tapes. In addition, flowing in the tangential direction



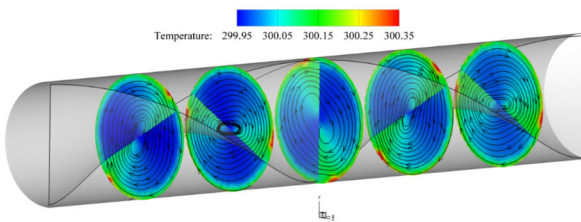
(a) schematic of a tube with twisted insert



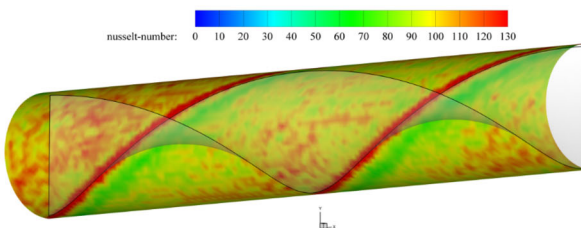
(b) grid generation of tube with a twisted tape insert



(c) streamline around the tube with twisted tape insert



(d) streamline and temperature field



(e) localNusselt number

Fig. 1 Contour plot of velocity and temperature field in a tube fitted with twisted tape

is observed. The contour plot of streamline and temperature field in Fig. 1d shows that swirl flows generated from twisted tapes along the tube could increase the homogeneous temperature. Obviously, the low-temperature fields and high Nusselt number appear in the contact zone of the flowing fluid at tape edge and tube wall affected by tangential contact between them, which is associated by swirl flow.

5.2 Axial Nu Distribution

The effect of twisted tape insert with TiO₂/water nanofluid on local heat transfer (Nu) along the tube length at Reynolds number ca 5400, 10,300 and 15,200 is presented in Fig. 2. A high local Nusselt number was observed at low x/D due to the sudden change of temperatures in the entry region. When increasing x/D , the Nusselt number exponentially decreased to the fully developed value and then slightly increased at the end of tube. The slight increase of Nusselt number at the end of tube was attributed to slightly increase in temperature due to the increase in friction. The TiO₂ nanoparticles suspended in water with twisted tapes were much outperformed the plain tube with pure water for heat transfer as seen from Nusselt number. Increasing concentration of TiO₂ nanoparticles could improve heat transfer, which may attribute to higher contact area between nanoparticles for transferring heat. This effect was especially more pronounced at high Reynolds number.

5.3 Heat Transfer

Figure 3 shows that inserting twisted tapes could enhance over 1.3–1.5 times heat transfer than the plain tube in a range of Reynolds number between 5400 and 15,200. It can be inferred that twisted tapes generated continuous swirling flow resulting in well transferring heat in the tube. Increasing Reynolds number would decrease Nusselt number due to the strong turbulence being dominant over swirling flow. In addition, the twisted tape insert with TiO₂ nanoparticles at $\phi = 0.07\%$, 0.14% and 0.21% by volume is augmented 41.7%, 43.9% and 47.1% higher Nusselt number when compared with the plain tube. As compared to the tube inserted twisted tape with pure water, TiO₂ nanoparticles/water in the tube inserted twisted tape is more effective, in that Nusselt number ratio was 1.03, 1.05 and 1.07 times for TiO₂ concentration at $\phi = 0.07\%$, 0.14% and 0.21% by volume, respectively.

5.4 Friction Factor

Figure 4 demonstrates the influences of concentration of TiO₂/water nanofluid (0.07 to 0.21% by volume) on friction factor characteristics. Friction was caused by the twisted tape insert which perturbed the flows within the tubes, as seen from Fig. 4a. It also shows that the tapes with larger concentration of nanofluid (ϕ) yielded higher friction factors. The friction factors obtained from the twisted tape insert with the $\phi = 0\%$ (pure water), 0.07% , 0.14% and 0.21% by volume, are 0.92 times, 0.92 times, 0.94 times and 1.08 times of those the plain tube, respectively. The friction factor ratio

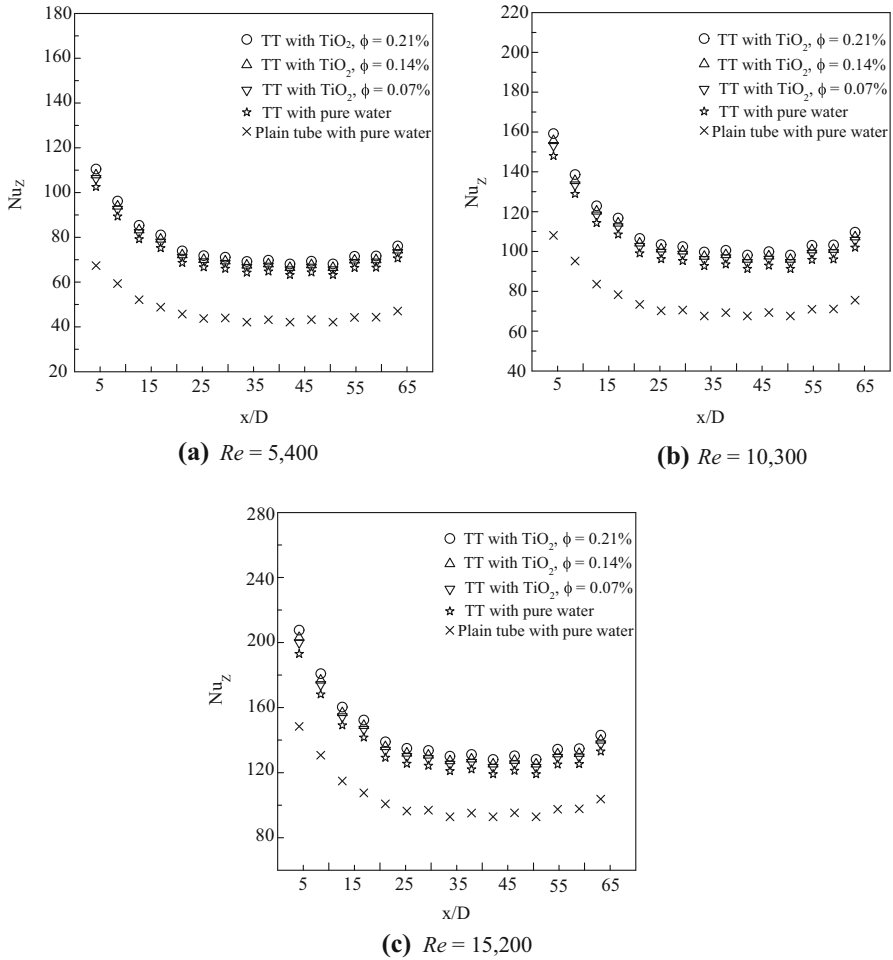


Fig. 2 Local Nusselt number distribution in a tube with twisted tape and nanofluid. Error for each point $\leq 5\%$

(f_i/f_p) slightly increased with increase in Reynolds number. This was attributed that a stronger turbulence affects to a higher dissipation of a dynamical pressure and thus an efficient heat transfer. Figure 4b shows that friction factors generated by twisted tape insert with nanofluid as compared to twisted tape insert with pure water are directly related to the result of fluid viscosity and shear force on tube wall acted by TiO_2 nanoparticles. The twisted tape with TiO_2 concentrations of 0.07%, 0.14% and 0.21% caused 9.3%, 11.2% and 14.2% higher friction factor than that with pure water, respectively. It is apparent that a higher TiO_2 concentration, especially 0.21%, was much more friction loss.

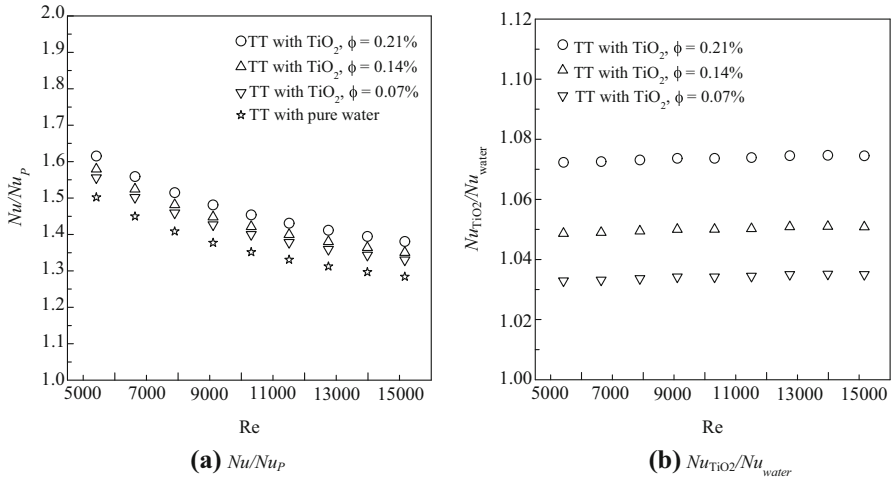


Fig. 3 Relationship between Nusselt number ratio and Reynolds number for tube with twisted tape and nanofluid. Error for each point $\leq 5\%$

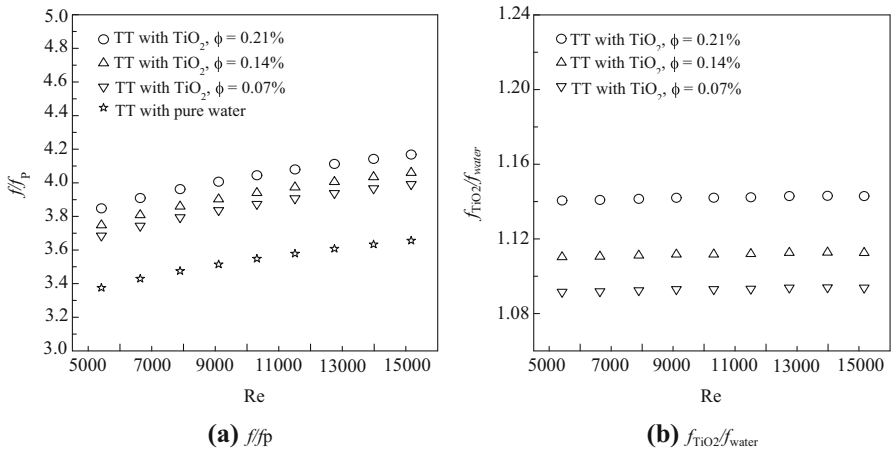


Fig. 4 Relationship between friction factor ratio and Reynolds number for tube with twisted tape and nanofluid. Error for each point $\leq 5\%$

5.5 Thermal Performance Factor

Figure 5 shows the variation of the thermal performance factor (η) with Reynolds number for all twisted tape insert with TiO_2 /water nanofluid. The thermal performance factor is considered under constant pumping power. The thermal performance factor tends to decrease with the increase in Reynolds number due to the increased friction factor ratio and the decreased Nusselt number at a turbulent flow regime. It is also observed that the thermal performance factor increased as concentration of nanofluid (ϕ) increased. The twisted tape insert with the $\phi = 0.07\%$, 0.14% and 0.21% by volume yielded thermal performance factors from 0.84 to 1.00, 0.85 to 1.02 and 0.86 to

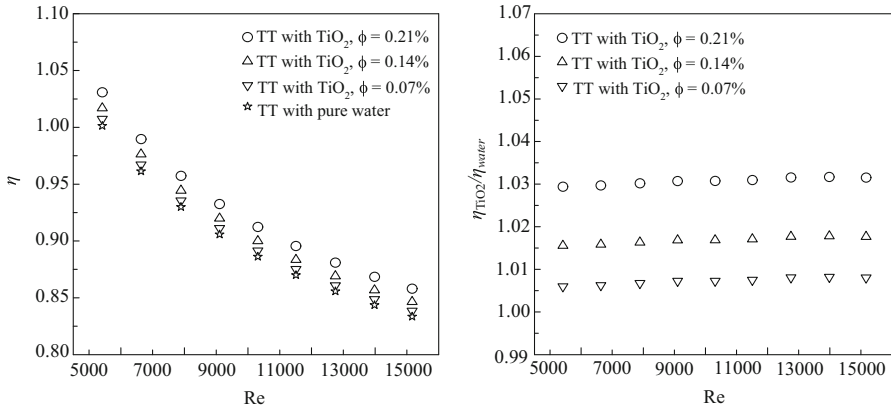


Fig. 5 Relationship between thermal performance factor and Reynolds number for tube with twisted tape and nanofluid. Error for each point $\leq 5\%$

1.03, respectively. Moreover, the thermal performance factor ratio in Fig. 5b indicated that the twisted tape insert with TiO_2 nanoparticles in water can be applied effectively, as seen from the value of thermal performance factor ratio more than unity. That is, thermal performance factors given by twisted tape insert with the $\phi = 0.07\%$, 0.14% and 0.21% by volume are higher than those provided by the twisted tape insert with pure water around 0.7% , 1.7% and 3.1% .

5.6 Empirical Correlations

From the experimental results, Nusselt number (Nu), friction factor (f) and thermal performance factor (η) are fitted and analyzed by least-square regression. The resultant correlations are shown in the following equations.

Nusselt number correlation:

$$Nu = 0.173Re^{0.618}Pr^{0.4}(1 + \phi)^{0.368} \tag{20}$$

Friction factor correlation:

$$f = 0.983Re^{-0.234}(1 + \phi)^{0.77} \tag{21}$$

Thermal performance factor correlation:

$$\eta = 4.598Re^{-0.178}(1 + \phi)^{0.111} \tag{22}$$

These correlations are subject to the evaluation of their reliabilities. The deviations for Nusselt number, friction factor and thermal performance factor are within $\pm 3\%$, $\pm 3\%$ and $\pm 1\%$, respectively, as shown in Fig. 6a–c.

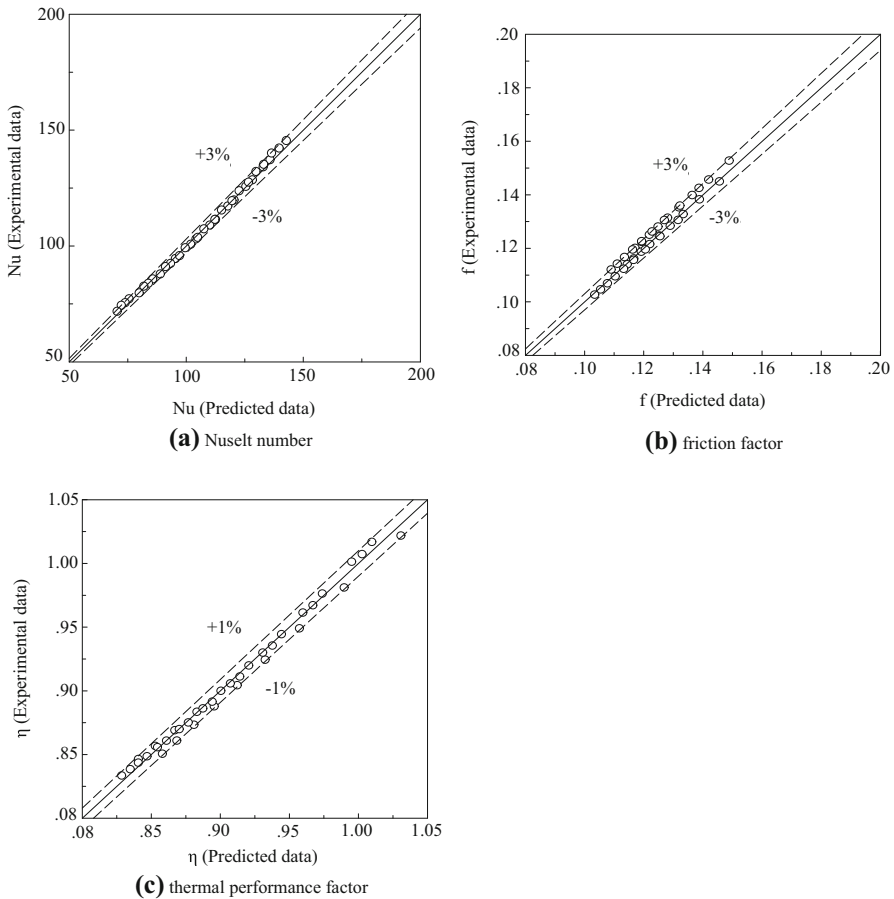


Fig. 6 Predicted data versus experimental data of tube with twisted tape and nanofluid

5.7 Stability of the Nanofluid

SEM image in Fig. 7a shows that the morphology of starting TiO_2 is a defined sphere-like structure. The aggregation and sedimentation phenomena of nanofluid were not found during the experiment. This was attributed that the sonication process can keep a good stability of TiO_2 over a long time during the experiment. After the experiment, TiO_2 particles can remain in suspension for more than 3 days. Closer inspection of used TiO_2 particles is presented by SEM image in Fig. 7b. It is apparent that the particle morphology of TiO_2 was retained during fluid flow, and TiO_2 aggregates were not present.

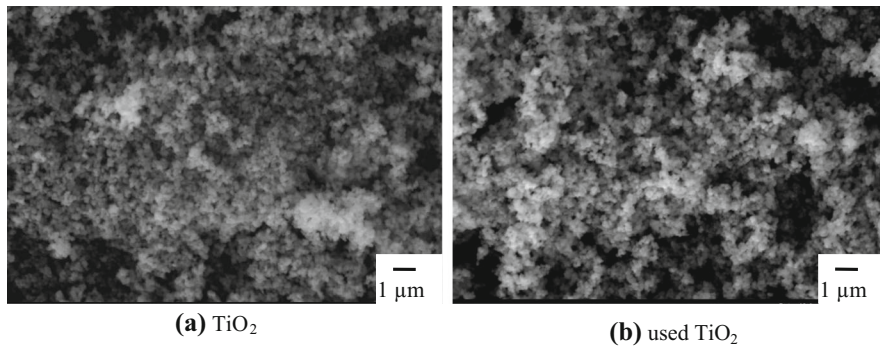


Fig. 7 SEM image of (a) TiO₂ and (b) used TiO₂

6 Summary

The twisted tape could generate the swirl flow around the tape, resulting in the homogeneous temperature. TiO₂ nanoparticles suspended in water played an important role in enhancing thermal conductivity and collision, and therefore outperformed the pure water for heat transfer as seen from an increasing Nusselt number. The Nusselt number was fully developed when increasing x/D and Reynolds numbers. The twisted tape insert with TiO₂/water nanofluid also yielded friction factor and thermal performance than the twisted tape insert with pure water. With a higher concentration of TiO₂ nanoparticles, the heat transfer, friction factor and thermal performance would be more pronounced. The twisted tape insert with 0.21 % *v/v* TiO₂ nanoparticles/water could achieve the highest performance factor up to 1.03, and Nusselt number and friction factor increased by 44.2 % and 294 % over that of the plain tube.

Acknowledgments Financial supported by the Thailand Research Fund and Office of the Higher Education Commission (Grant No. MRG6180262) are gratefully acknowledged.

References

1. S. Jaisankar, T.K. Radhakrishnan, K.N. Sheeba, *Sol. Energy* **83**, 1943–1952 (2009)
2. S. Jaisankar, T.K. Radhakrishnan, K.N. Sheeba, *Energy* **34**, 1054–1064 (2009)
3. S. Bhattacharyya, S.K. Saha, *Exp. Therm Fluid Sci.* **42**, 154–162 (2012)
4. S. Saha, S.K. Saha, *Exp. Therm. Fluid Sci.* **47**, 81–89 (2014)
5. P. Sivashanmugam, S. Suresh, *Chem. Eng. Process.* **46**, 1292–1298 (2007)
6. J. Guo, M. Xu, L. Cheng, *Chem. Eng. Process. Process Intensif.* **49**, 410–417 (2010)
7. M.M.K. Bhuiya, M.S.U. Chowdhury, J.U. Ahamed, M.J.H. Khan, M.A.R. Sarkar, M.A. Kalam, H.H. Masjuki, M. Shahabuddin, *Int. Commun. Heat Mass Transfer* **39**, 818–825 (2012)
8. M.M.K. Bhuiya, J.U. Ahamed, M.S.U. Chowdhury, M.A.R. Sarkar, B. Salam, R. Saidur, H.H. Masjuki, M.A. Kalam, *Int. Commun. Heat Mass Transfer* **39**, 94–101 (2012)
9. K. Nanan, C. Thianpong, P. Promvongse, S. Eiamsa-ard, *Int. Commun. Heat Mass Transfer* **52**, 106–112 (2014)
10. L. Syam Sundar, M.K. Singh, *Rev. Renew. Sustain. Energy Rev.* **20**, 23–35 (2013)
11. M.J. Assael, I.N. Metaxa, K. Kakosimos, D. Constantinou, *Int. J. Thermophys.* **27**, 999–1017 (2006)
12. G.A. Longo, C. Zilio, *Int. J. Thermophys.* **34**, 1288–1307 (2013)
13. K.V. Sharma, L.S. Sundar, P.K. Sarma, *Int. Commun. Heat Mass Transfer* **36**, 503–507 (2009)

14. L.S. Sundar, K.V. Sharma, *Int. J. Heat Mass Transfer* **53**, 1409–1416 (2010)
15. M.T. Naik, G.R. Janardana, L.S. Sundar, *Int. Commun. Heat Mass Transfer* **46**, 13–21 (2013)
16. S. Suresh, K.P. Venkitaraj, P. Selvakumar, *Superlattices Microstruct.* **49**, 608–622 (2011)
17. S. Suresh, K.P. Venkitaraj, P. Selvakumar, M. Chandrasekar, *Exp. Thermal Fluid Sci.* **39**, 37–44 (2012)
18. K. Wongcharee, S. Eiamsa-ard, Enhancement of heat transfer using CuO/water nanofluid and twisted tape with alternate axis. *Int. Commun. Heat Mass Transfer* **38**, 742–748 (2006)
19. S. Eiamsa-Ard, K. Wongcharee, *Int. Commun. Heat Mass Transfer* **39**, 1453–1459 (2012)
20. K. Wongcharee, S. Eiamsa-ard, *Int. Commun. Heat Mass Transfer* **39**, 251–257 (2012)
21. Y. He, Y. Jin, H. Chen, Y. Ding, D. Cang, H. Lu, *Int. J. Heat Mass Transfer* **50**, 2272–2281 (2007)

Publisher's Note Springer Nature remains neutral with regard to jurisdictional claims in published maps and institutional affiliations